BEAM DYNAMICS STUDIES OF A HIGH-REPETITION RATE LINAC-DRIVER FOR A 4TH GENERATION LIGHT SOURCE *

M. Venturini†, J. Corlett, P. Emma, C. Papadopoulos, G. Penn,
M. Placidi, J. Qiang, M. Reinsch, F. Sannibale, C. Steier, C. Sun, and R. Wells
LBNL, Berkeley, CA 94720 USA

Abstract

We present recent progress toward the design of a superconducting linac driver for a high-repetition rate FEL-based soft x-ray light source. The machine is designed to accept beams generated by the APEX photo-cathode gun operating with MHz-range repetition rate and deliver them to an array of SASE and seeded FEL beamlines. We review the current baseline design and report results of beam dynamics studies.

INTRODUCTION

An on-going R&D program at LBNL is dedicated to the goal of designing a 4th generation light source in the 0.27 − 1.2 keV spectrum range (in the fundamental) making use of a high-repetition rate photo-gun injector to feed an array of FEL beamlines operating in the SASE, self-seeded, and externally seeded modes [1]. A prototype of the injector, based on the APEX gun is presently under construction [2], promising to generate high-brightness electron bunches with charge up to 1 nC and repetition rate of few MHz's. In this paper we report on progress toward the design of a linac driver that would accept bunches from the APEX injector and deliver them to the FELs with the desired peak current and minimal degradation of the beam brightness.

The specifications of the baseline design are summarized in Table 1. The choice of beam energy is compatible with generation of significant radiation power in the 3rd and 5th harmonics and use of superconducting undulators with $\lambda_u = 19.4$ mm period. The maximum 300 pC charge/bunch is primarily defined by the desire to limit the heat load on the rf structures (at 1 MHz). The transverse beam brightness and peak current are specified to yield 10^{11} photons/pulse in the SASE mode at 1.2 keV and up to 10^{12} photons/pulse at lower energies, while the demand on the slice energy spread is set by the operation of self- and externally seeded beamlines.

The main known factor contributing to growth in the slice energy spread is the microbunching instability. The desire to minimize the microbunching instability would offer a compelling motivation to opt for one-stage magnetic compression in the linac and indeed single bunch-compressor lattices were considered in our previous studies [3, 4]. However, in the present design we propose a lattice that in its main mode of operation would utilize two

Table 1: Selected Beam Parameters at the FEL

Energy	2.4 GeV
Charge/bunch	300 pC
Beam power	$\leq$ 0.72 MW
Slice rms emittance $\gamma\varepsilon_\perp$	0.6 μm
Slice energy spread (bunch core)	150 keV
Current (bunch core)	$\geq$ 600 A

bunch compressors. While this choice appears to be consistent with the energy-spread specifications, care was taken to make the machine layout sufficiently versatile to operate in a single-stage compression mode as well.

The beam high power enabled by the high-repetition rate injector can only be supported by superconducting rf structures. In developing the machine design we are tentatively adopting a basic cryomodule unit based on the TESLA 1.3 GHz cavity design, with a choice of 7 cavities per module. The flexibility to operate the machine on a range of bunch charges (possibly down to few 10s of pC) is an intended but still untested feature. Likewise, still unexplored is the interesting possibility of operating the machine with different bunch charges simultaneously.

MACHINE DESIGN

The machine layout contains all the basic elements one expects from an accelerator driver of an x-ray FEL. Following the injector (beam energy in the 84-100 MeV range), a small chicane hosting the laser heater, and a 6D diagnos-

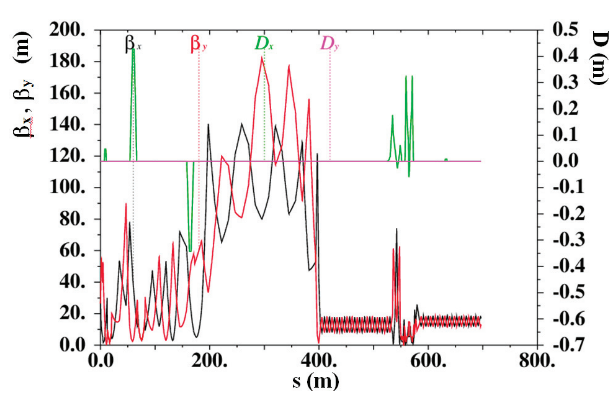

Figure 1: Lattice functions from the exit of the injector through the linac, including switchyard, branchline, and the self-seeded FEL beamline through the last undulator.

* Work supported by DOE under Contract No. DE-AC02-05CH11231.
† mventurini@lbl.gov

ISBN 978-3-95450-115-1

Table 2: Basic Machine Settings

Section	$V_{\rm rf}$ (MV)	$\phi_{\rm rf}$ (deg)	R_{56} (m)
L1	111	-30.3	
BC1			-0.075
L2	474	-30.5	
BC2			-0.049
L3	1718	14.1	

tics section, the beam is accelerated through the first accelerating section L1 into the first bunch compressor (BC1) to about 200 MeV, with a third-harmonic cavity linearizer positioned right before BC1. The second accelerating section (L2) leads to BC2 at about 700 MeV beam energy, and finally L3 accelerates the beam up to 2.4GeV. Fast kickers distributed along the switchyard (see [5]) direct the beam into up to 10 identical curved branchlines, each feeding a separate FEL. The FEL beamlines are parallel to each other and at a 36 deg angle with respect to the linac axis. Selected machine parameter settings are reported in Table 2.

Efficient operation of the laser heater favors a beam energy at the high end of the energy range accessible by the proposed injector. Using the same $\lambda_L = 1064$ nm laser wavelength driving the APEX the photo-gun, about one μJ laser pulses will be needed (averaging to 1 W power at 1 MHz) to induce up to 12 keV slice energy spread (rms).

The present design makes a conservative assumption of about 14 MV/m maximum accelerating gradient over a cavity active length, requiring a total total of 26 cryomodules in the linac (excluding the module for the linearizer).

The values of the lattice functions at the end of the bunch compressor chicanes are optimized to reduce the CSR-induced projected emittance growth. While the projected emittance growth through the end of the machine remains modest, further lattice optimization involving fine tuning of the phase advances between the dispersive regions may still be possible. The relatively large beta functions through L3 (see Fig. 1) are intended to reduce the magnitude of the microbunching instability, which is dependent on the transverse beamsize, and hence the energy spread growth past the second bunch compressor. Their value was not found to have adverse consequences on the dynamics (*e.g.* by impacting emittance through chromatic effects).

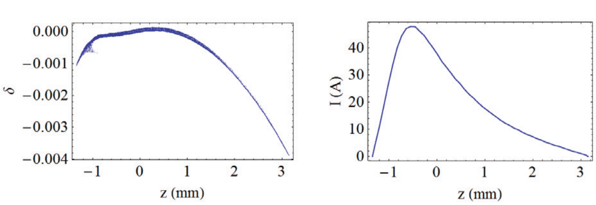

Figure 2: Example of beam longitudinal phase space (left) and current profile at the exit of the injector. The bunch head on the left. (ASTRA simulations).

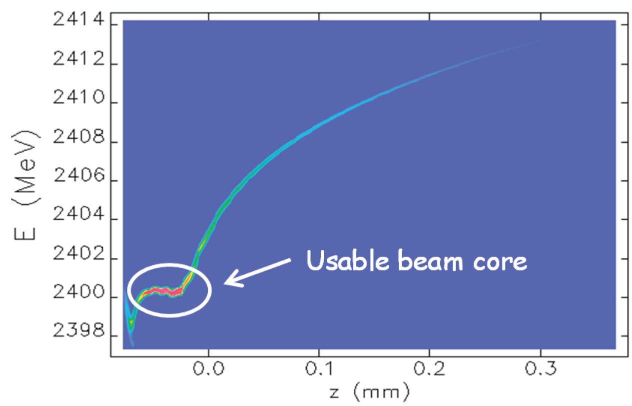

Figure 3: Beam longitudinal phase space at the entrance of the FEL beamlines. (Elegant simulations.)

BEAM DYNAMICS SIMULATIONS

The relatively small accelerating field in the APEX gun prevents the current at the cathode from being much higher than about 5 A without compromising the transverse brightness. As a result, the bunches need to undergo more than a factor 100 compression before they can be used in the FELs. We partition the overall compression about equally between rf (occurring in the injector, see [6]) and magnetic (taking place along the linac) compression. A significantly larger magnetic compression would be problematic as the energy chirp after the last chicane would become difficult or expensive to remove. On the other hand, rf compression larger than about a factor 10 would degrade the transverse emittance and cause excessive distortions in the longitudinal phase space (in turn, further limiting magnetic compression downstream). Rf compression introduces some peculiar features in the beam characteristics, most notably an asymmetric current profile presenting a long and relatively well populated tail and potentially large nonlinear correlations in the longitudinal phase space. Both features have implications on the downstream dynamics and affect the characteristics of the beam at the exit of the machine.

A typical beam at the exit of the APEX injector, used in the simulations discussed here, with about 50A peak current, 0.73 μm projected (and less than 0.6 μm slice) transverse emittance is shown in Fig. 2. The corresponding longitudinal phase-space at the entrance of the FEL beamlines as simulated with the code Elegant [7] is shown in Fig. 3. At the entrance of the FEL beamlines the usable core of the beam, with acceptably uniform energy and instantaneous current between 600 A and 1 kA, is about 140 fs long and accounts for about half the bunch charge. The rest of the bunch charge is mostly in a long low-current tail with energy significantly different from the nominal. Magnetic compression between BC1 and BC2 is roughly split in the $3 \div 4.5$ ratio. Further magnetic compression is prevented by occurrence of current spikes (the incipient development of these spikes is already apparent at the edges of the beam

ISBN 978-3-95450-115-1

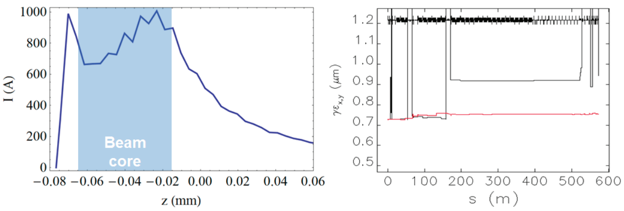

Figure 4: Beam current profile (left) and evolution of the projected transverse rms emittances along the machine.

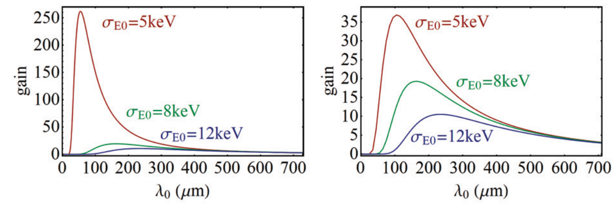

Figure 6: Gain for the microbunching instability from the injector through the last compressor for two-stage (left) and one-stage compression.

core, as seen in the left picture of Fig. 4) and difficulty with energy chirp removal from the beam core. The energy chirp from the beam core is removed by a combination of dephasing L3 by about 14 deg off-crest, the contribution of the rf wakes in L3, and most importantly, the contribution of the CSR longitudinal wakefields, primarily from three strong (10 deg) dipoles in the curved branchlines following the spreader. Interestingly, the machine setting yielding the Fig. 3 beam does not require powering the linearizer. An effective cancelation of the quadratic chirp within the usable beam core results from the rf wakefields in L1 and L2, and CSR wakefields in the bunch compressors, and a relatively low overall compression factor. However, in single-stage compression mode, a linearizer with 20 MV voltage is found to be beneficial for the attainment of the nominal current along the beam core. The present machine design includes a 7-cavity 3.9 GHz linearizer module capable of supporting up to 30 MV voltage. The results of the simulations shown here are for an ideal, error-free lattice ignoring possible effects from transverse wakefields as well as multibunch interactions.

Inspection of the longitudinal phase space (Fig. 3) shows the presence of a small but noticeable energy modulation which we attribute to microbunching instability driven by CSR, perhaps enhanced by the limited number of macroparticles (250k) used in the Elegant simulations. In these simulations the main driver of the microbunching instability, longitudinal space charge, was intentionally turned off. Instead, for an accurate study of the instability we resort to the IMPACT code [8], implementing a fully 3D model of space charge, capable of handling multi-billion macroparticles and therefore less exposed to spurious numerical effects. Simulations using IMPACT show that with

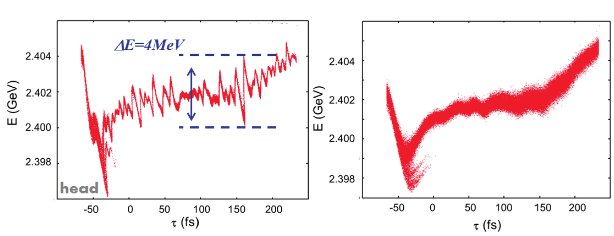

Figure 5: Longitudinal phase-space of the beam core at the exit of the spreader with laser heater off (left) and on. (IMPACT simulations.)

the laser heater off the beam would experience strong microbunching (Fig. 5, left picture). Effective damping can be achieved by a setting of the laser heater inducing about 10 keV rms energy spread (Fig. 5, right picture). The microbunching instability modeled in these simulations was seeded by shot noise; other possible sources (*e.g.* noise in the laser driving the photo-gun) will be included in the future for a more accurate assessment. The instability gains from linear theory reported in Fig. 6 contrast the one-stage and two-stage compression lattices showing the possible advantage of performing one-stage compression.

CSR is included through the 1D model implemented in Elegant and IMPACT. Care has been taken to account for CSR over an appropriate distance in the drifts downstream each dipole to capture transient effects. The growth found in the projected horizontal emittance is minimal through BC1, raises through BC2, and experiences only modest further growth through the spreader (right picture in Fig. 5). As expected, we did not observe growth in the slice emittance as there are no mechanisms in the dynamics model that could cause any changes. 3D CSR effects, which have the potential to affect the slice emittance will be assessed in future studies. Operating the machine in the one-stage compression mode (with the energy of the beam at BC1 raised to 280MeV and suitable readjustment of the Twiss functions) causes the overall projected emittance to grow to about 1.2 μm, while keeping the compression about the same as in the baseline setting.

Preliminary start-to-end simulations through the SASE beamline using the combinations of ASTRA-Elegant-Genesis and IMPACT-Genesis codes show results consistent with the performance goals.

REFERENCES

[1] J. Corlett et al., these Proceedings.
[2] F. Sannibale et al., these Proceedings.
[3] M. Venturini et al., PAC11 Proceedings, (2011).
[4] E. Kurr et al., LBNL Report LBNL-2670E, (2009).
[5] M. Placidi et al., these Proceedings.
[6] C. Papadopoulos et al., these Proceedings.
[7] M. Borland, Elegant, Advanced Photon Source LS-287, (2000).
[8] J. Qiang et al., J. Comp. Phys **163** 434, (2000).

ISBN 978-3-95450-115-1